

Integrity of H1 helix in prion protein revealed by molecular dynamic simulations to be especially vulnerable to changes in the relative orientation of H1 and its S1 flank *

Chih-Yuan Tseng^{1†}, Chun-Ping Yu¹ and HC Lee^{1,2}

¹Department of Physics and ²Graduate Institute of Systems Biology and Bioinformatics
National Central University, Chungli, Taiwan 320

Abstract

In the template-assistance model, normal prion protein (PrPC), the pathogenic cause of prion diseases such as Creutzfeldt-Jakob (CJD) in human, Bovine Spongiform Encephalopathy (BSE) in cow, and scrapie in sheep, converts to infectious prion (PrPSc) through an autocatalytic process triggered by a transient interaction between PrPC and PrPSc. Conventional studies suggest the S1-H1-S2 region in PrPC to be the template of S1-S2 β -sheet in PrPSc, and the conformational conversion of PrPC into PrPSc may involve an unfolding of H1 in PrPC and its refolding into the β -sheet in PrPSc. Here we conduct a series of simulation experiments to test the idea of transient interaction of the template-assistance model. We find that the integrity of H1 in PrPC is vulnerable to a transient interaction that alters the native dihedral angles at residue Asn¹⁴³, which connects the S1 flank to H1, but not to interactions that alter the internal structure of the S1 flank, nor to those that alter the relative orientation between H1 and the S2 flank.

Key words: Prion, Template-assistance model, Transient interaction, Molecular dynamics simulation

1 Introduction

Prion protein (PrP) in its infectious form is the pathogen that causes several prion diseases such as Creutzfeldt-Jakob (CJD) in human, Bovine Spongiform Encephalopathy (BSE) in cow, and scrapie in sheep [30]. Two reviews recently summarize past studies and discuss molecular mechanisms of the prion disease to understand physiological function of PrP and pathogenic pathways [1, 2].

An *in vitro* experiment conducted by [7] provides strong evidence for the protein-only hypothesis. Fig. 1 shows an NMR structure of the C-terminal of mouse PrP in its native form (PrPC) (PDB code: 1AG2). It contains 103 residues from Gly¹²⁴ to Tyr²²⁶ classified into secondary structures and surface loops [31]. These include three α -helices: H1, residues 144 to 152, H2 (173-193), and H3 (200-216); two β -strands: S1 (129-131) and S2 (161-163), which form an anti-parallel β -sheet; six loops: L1 (124-128), L2 (132-143), L3 (153-160), L4 (164-172), L5 (194-198), and L6 (217-226). In what follows we shall refer to the S1-L2 segment as the S1 flank, or F1, the L3-S2 segment as the S2 flank (F2), and the segment from S1 to S2, inclusive, as the S1-H1-S2 peptide. Homologues of PrP in other organisms generally have residue numbering that differ from the mouse numbering given in Fig. 1; unless explicitly otherwise specified, in this text we will use the mouse numbering.

Fig. 1 is here.

*This paper has been accepted for publication in European Biophysical Journal on Feb 2, 2009.

†Present address: Department of Oncology, University of Alberta, Edmonton, AB T6G 1Z2 Canada. E-mail: chih-yuan.tseng@ualberta.ca; richard617@gmail.com

Experimental investigations suggest that the pathogenicity of prion diseases is characterized by the unfolding of PrPC followed by misfolding into the infectious scrapie isoform (PrPSc) [29], which involves conformational changes in the C-terminal residues 121-231 but no chemical reaction [16, 18]. Muramoto et al. showed the H2 and H3 helices seem to be stabilized by disulfide bonds and likely to have the same conformation in PrPC and PrPSc [27]. They also found the deletion of both H2 and H3 from PrPC does not stop its conversion to PrPSc. Eghiaian et al. showed the epitope of antibody to be conserved in the H2 and H3 regions, again suggesting that these two helices are conserved during conversion [13].

Because the H2-H3 region seems to be conserved during the PrPC to PrPSc conversion, recent experimental and computational investigations have focused on the S1-H1-S2 region (residue 124 to 163), and these have revealed important features of the prion disease. A predominantly helical propensity in the H1 region is demonstrated by several *in silico* studies under different experimental conditions by [33] and [34]. On the question of possible mechanisms that trigger the conformational conversion, *in vitro* studies suggest that altering the pH level of the solvent, which varies static electric interactions, might destabilize the H1 helix and trigger conversion [39, 5]. Similar effects were observed in *in silico* studies by [21], [22] and by [9]. In simulations on mouse prion 1AG2, Guilbert et al. found that a major modification of dihedral angles around the residue 125 was required for the formation of a β -strand in residues 121-133 [15]. In addition, DeMarco and Daggett show detachment of the S1-H1-S2 region from the rigid H2-H3 region to accommodate misfolding and the H1 helix is only partially unfolded [10]. By studying the isolated S1-H1-S2 peptide, Sharman et al. and Ziegler et al. both showed a predominantly helical propensity in the H1 region for PrP in water as well using CD and NMR methods [35, 40]. This property is further demonstrated by Dima and Thirumalai's [12] and by Watzlawik et al.'s studies [37]. When Watzlawik et al. experimentally clarified role of the H1 helix in the conversion, they found the H1 helix does not convert into β -sheet yet it promotes aggregation. In addition, Kozin et al. found that residues 142-166 in human numbering (same numbering as in mouse) has the propensity to form a β -hairpin around residues 153-156 at neutral pH level as well [20], which they believe to be the event that drives the conversion. In addition, Derreumaux showed the residues 127-164 region has two equi-energetic conformations with β or α features [11]. Megy et al. provide an experimental evidence for this structural duality [25]. They found the β structure in the region spanning residues from 142 to 167 very similar to NMR spectroscopy β structure. These results may be summarized as follows: in the PrPC to PrPSc conversion the S1-H1-S2 region plays an important role while the H2-H3 region plays at most a passive role, and during the conversion the β -sheet breaking in PrPC is likely to be the first barrier [3] and detachment of the S1-H1-S2 region from the rigid H2-H3 region is another barrier [10]. The H1 helix is only partially unfolded. Thus, here we only aimed to study H1 stability using the S1-H1-S2 peptide.

One of the models advanced for the pathogenesis of the prion disease is the template-assistance model [30, 17, 36]. In this model it is assumed that PrPC, normally more stable than PrPSc in isolation, would in the presence of PrPSc convert to the latter via a transient catalytic interaction with it. The implication is that a dimer of PrPSc's is energetically more stable than a system of non-interacting PrPC and PrPSc, which was confirmed by Morrissey and Shakhnovich's computational analyses [26]. When there are other PrPC present, the initial autocatalytic process would then lead to a propagation of PrPC to PrPSc conversion. Because PrPSc's always appear in aggregated state and not in isolation, its structure is not precisely known at present [9, 20], rendering an investigation of the conversion-causing transient interaction between PrPC and PrPSc problematic. Nevertheless, an in-principle feasibility of the template-assistance model was demonstrated by Malolepsza et al. [24]. In their computer simulations the PrPSc was approximated by peptides with β -sheet structure, and the authors found that such peptides were able to induce conversion of peptides with α -helix.

A key assumption of the template-assistance model is that the the PrPC to PrPSc conversion is triggered by a transient interaction, as opposed to, say, a series of slow-acting contacts. Here, we use computer simulation to explore possible consequences of transient interactions that may

trigger the PrPC to PrPSc conversion, without explicitly including the latter in the simulation. In practice, we investigate what sudden changes to the conformation of PrPC would destabilize its native structure. If a conversion triggering transient interaction is found, then a possible next step is to see whether (in simulation) the presence of a PrPSc in the vicinity of a PrPC indeed would affect such an interaction. We take a two-step approach because a general exploration of possible transient interactions between PrPC and PrPSc by MD simulation would exceed our present computational capability, and because an accurate knowledge of the conformation of PrPSc is lacking.

As mentioned in [1], a clear understanding of the physiological function of the PrPC and its interaction partner is still lacking, and this in turn prevents us from understanding the roles PrPC and PrPSc play in the pathogenesis of prion diseases. Thus, in the present work we institute structural changes in PrPC *by hand*, changes that we assume may be caused by hypothetical transient interactions, and follow the aftermath in each case by molecular dynamics (MD) simulation. Our goal is to investigate the dynamics of structural modifications of PrPC under simulations. Specifically we focus on the stability of H1 after a change made in the S1-H1-S2 peptide (residues 124-167). Our study contains two parts. In the first part we attempt to determine changes in which one of the two flanks - F1 and F2 - is more likely to initiate an unfolding of H1. We find the answer to be F1. In the second part, we initiate specific structural changes in F1, run MD simulations on the S1-H1-S2 peptide, and focus our attention on the way H1 is affected. We find the native structure of the S1-H1-S2 peptide to be generally quite robust. Among structural alterations made to F1, modification of the two dihedral angles of Asn¹⁴³ is found to be most likely to lead to the unfolding of H1, and that when H1 unfolds, it tends to form a β -hairpin turn at residues 150-152, which is close to the 153-156 region reported in [20]. Our results also suggest that hydrophobic forces do not play a major role in the conversion process.

2 Method

2.1 Simulation parameter settings

The simulation package AMBER 8 [6] is used for energy minimization and MD simulation with the AMBER force field ff03. As a prelude to each simulation a full conjugate gradient energy minimization is applied for 1000 iterations to allow the spatial positions of the atoms to relax to their respective local energy minima. During minimization and MD simulation SHAKE [32] is invoked to constrain hydrogen bonds. This has the effect of preventing the fast bond vibration motion of hydrogens. The cut-off distance for non-bonded interactions in all calculations is set to be 15 Angstrom.

For the MD simulation, system temperature is at room temperature, or 300 K. Andersen temperature coupling is employed to regulate temperature between protein and the environment. Simulation time step is 2 fs. Initial velocities of atoms in proteins are generated from Boltzmann distributions at 300 K temperature. The effect of solvent is represented by the modified generalized Born model of Onufriev et al. [28], where the pH is set to neutral, and where, for calculating the effective Born radius, the maximum distance between a pair of atoms is set to be 12 Angstrom. Periodic boundary condition is not applied in the calculations. The cut-off distance of non-bonded interactions is set to be 15 Angstrom.

The MD simulations are performed on a 32-node PC cluster at the National Center for High-performance Computing in Taiwan. Under the above settings the average CPU time needed to simulate the folding of a 40-amino-acid peptide for 1 ns is about half an hour.

2.2 Designs for two series of simulations on S1-H1-S2

Our intention is to represent the effect of potential conversion-triggering transient interactions on the S1-H1-S2 peptide (residues 124 to 167) by artificially induced structural changes to the peptide,

and study the stability of the affected peptide through MD simulation. Following this strategy we carry out two series of exploratory simulations classified according to the artificial changes made to the peptide and designated $Enfm$, where $n=1$ and 2 is the classifier, and m enumerates the simulations in each class. In practice, a specific designation indicates a specific initial conformation for the peptide. In addition, $f0$ (without the prefix En) denotes the benchmark simulation in which the S1-H1-S2 peptide has the native conformation as its initial conformation.

The E1 series. The goal of this series of simulations is to identify which flank, F1 or F2, plays a crucial role in the stability of H1. We consider three extreme cases. In each case, either F1, F2, or both together, is completely pruned from the S1-H1-S2 peptide and the remainder, initially in its respective native conformation, is simulated. In E1f1, F2 is pruned and the remainder consists of residues 124 to 154. In E1f2, F1 is pruned and the remainder consists of residues 142 to 167. In E1f3, both flanks are pruned and the remainder consists of residues 142 to 154. When F1 is pruned, native contacts of mouse PrPC including the hydrogen bonds in the anti-parallel β -sheet, between the residue Arg¹³⁶ and the four residues Met¹⁵⁴, Tyr¹⁵⁵, Tyr¹⁵⁷, and Pro¹⁵⁸, and between residues Pro¹³⁷ and Tyr¹⁵⁰ are broken. In contrast no native contacts other than the hydrogen bonds in the anti-parallel β -sheet are broken when F2 is pruned. It indicates F1 plays a more important role in the stability of H1 than F2. This notion is discussed further in section 3. The total simulation time for this series is approximately 800 ns.

The E2 series. Guilbert et al. [15] pointed out that a major modification of the dihedral angles of a residue in F1 is required for the formation of a β -sheet on the S1-H1-S2 peptide. This, together with the result from the E1 simulations, mainly that F2 plays a minor role in the stability of H1 relative to F1, motivate the E2 simulations described below. In each simulation, the initial conformation of F2 relative to H1 is unchanged, and one of two types of changes is made on F1. In the first type, the dihedral angles of Asn¹⁴³, the residue joining F1 to H1, are changed. The native values of the dihedral angles are $\Phi_0 = -124.854^\circ$ and $\Psi_0 = 132.794^\circ$, which lie within the β -strand region in the Ramachandran plot. In three simulations, designated E2f1, E2f2 and E2f3, the initial values of (Φ, Ψ) are changed to $(\Phi, \Psi)_1 = (60^\circ, 60^\circ)$, $(\Phi, \Psi)_2 = (\Phi_0, 0^\circ)$, and $(\Phi, \Psi)_3 = (-60^\circ, \Psi_0)$, respectively, see Fig.2. These modifications are made using DeepView/Swiss-Pdb viewer [14]. Fig.2, as is Fig.1, are generated by Pymol [8]. In the Ramachandran plot, $(\Phi, \Psi)_1$ lies in the left-handed helical region, $(\Phi, \Psi)_2$ in the right-handed helical region, and $(\Phi, \Psi)_3$ in the β -strand region. The total time for the three simulations is about 1 μ s. In all initial conformations in the above E2 series runs, native contacts including the hydrogen bonds in the anti-parallel β -sheet, between the residue Arg¹³⁶ and the four residues Met¹⁵⁴, Tyr¹⁵⁵, Tyr¹⁵⁷, Pro¹⁵⁸, and between residues Pro¹³⁷ and Tyr¹⁵⁰ are broken. No new contacts are formed.

In the second type, for which only one simulation (E2f4) is run, the initial internal conformation of F1 is altered by changing the values of dihedral angles of Ser¹³⁵ from $\Phi = -75.575^\circ$ and $\Psi = 150.389^\circ$ to $\Phi = -75^\circ$ and $\Psi = 60^\circ$. This change has the effect of causing residues 124-143 to form a β -hairpin-like structure (right panel in Fig.2). In this case, only the hydrogen bonds in the anti-parallel β -sheet (in native mouse PrPC) are broken.

Fig. 2 is here.

2.3 In-house analysis tool

We employ several in-house tools to analyze the simulation results. The code PTRAJ from the AMBER package is used to extract peptide conformation at 1 ns intervals, and the program DSSP [19] to identify protein secondary structure. Two programs, g_sas and g_saltbr, from the MD package GROMACS [38, 4, 23] are used to calculate solvent accessible surfaces (SAS) and salt-bridge distances, respectively. We will use a similarity matrix to define a distance between two simulations. Confidence interval of the similarity thereafter is estimated using the maximum likelihood estimate.

3 Results

3.1 Results of the f0 simulation

Stability of the S1-H1-S2 peptide. The benchmark experiment f0, was simulated for 200 ns during which, at intervals of 1 ns, the conformation of the S1-H1-S2 peptide is extracted. In the simulation of S1-H1-S2 (in mouse), the S1-H1-S2 forms a stable conformation different from its native state characterized by two quantities, the root mean square deviation (RMSD) and radius of gyration, shown in Fig.3, but H1 remains largely intact. The RMSD calculates C_α atoms's positional difference between conformation in the simulation and the native conformation.

Although the RMSD in the left panel of Fig. 3 shows two drops around 50 and 175 ns, the average RMSD is around 11 Angstrom during the whole simulation. The radius of gyration indicates spatial extent of all C_α atoms. The right panel of Fig. 3 shows that the spatial extent of the structure remains stable after collapsing around 12 ns. One may attribute the collapse to the following reason. Barducci et al.'s studies suggest Tyr¹²⁸, Arg¹⁶⁴, and Asp¹⁷⁸ stabilize the β -structure in the S1-H1-S2 peptide [3]. Particularly, mutation of Asp¹⁷⁸ will severely cause disruption of the β -sheet. Thus one should expect unzipping of the β -sheet in our simulation because of absence of the Asp¹⁷⁸ in the initial conformation. As shown in Fig. 7 in next section there is the disruption of the β -sheet after 5 ns. In addition, there is a stable H-bonded turn around Met¹³⁸ formed after 1 ns for the whole simulation. These two reasons may result in the collapse of conformation.

Helical propensity in H1. The number of the residues from the H1 region - D¹⁴⁴WEDRYYR¹⁵¹ - forming the current α -helix is recorded at intervals of 1 ns in the 200 ns simulation. The result of the content variation along the simulation time is plotted in f0 panel of Fig. 4. Since it takes 3.6 residues to form a turn in an α -helix, one can define a zero-turn helix that consists of 0 to 2 residues, one full turn helix contains residue 3 to 5, and two full turns helix contains 6 to 8 residues. This coarse-grained description provides a simple way to account for helical structural variations. In the f0 simulation H1 has zero turn in 8 accumulative ns out of a total 200 ns, one full turn in 70 out of 200 ns, and two full turns in 122 out of 200 ns. There is a strong helical propensity in H1. These results are consistent with expectations [12].

Fig. 3 is here.

Fig. 4 is here.

3.2 Results of E1 simulations

Stability of H1 is more dependent on F1. The number of residues forming the α -helix in H1 region in E1f1, E1f2, and E1f3 is recorded. Each of the three simulations were run for 200ns. In each case, various data, including the number of residues forming the alpha-helix in H1 region (residue 144 to 152) were recollected at 50 ps intervals. The plots in Fig. 4 show the number of residues at every 20th data points, or effectively, data taken at 1 ns intervals. We will then apply a similarity analysis in the following to analyze the simulation results.

First, similarity of the f0 and the E1 simulations is defined as inner-product of two unit vectors, s . A vector characterized the simulation contains nine elements, which are accumulative times in 200 ns simulation of 0, 1,..., 8-residue in H1 forming a α -helix correspondingly. Then the unit vector is obtained by normalizing the vector by its length. The value of s ranges from 0 to 1. A zero inner product indicates the two vectors to be completely different and one denotes the two to be identical. Thus one obtains a four by four similarity matrix to reveal all correlations among the f0 and three E1 simulations S . Thereafter, we define a distance matrix, $D = 1 - S$ to reveal similarities among the simulations. Fig. 5 shows an example of a schematic plot of family tree. Notes that each end point of branch in the tree represents a simulation and then total branch's length between two end points denotes their differences. For example length between the f0 and the E1f1 $l_{f0-E1f1} = l_{f0-1} + l_{1-E1f1}$. Longer the branch's length is, the two simulations differ more. After twenty family trees corresponding to data recorded at different intervals are constructed, we apply the maximum likelihood estimate to evaluate confidence interval of length between two simulations. The 95 % confidence interval of length from the f0 to the E1f1 is $l_{f0-E1f1} = 0.1192 \pm 0.0114$

unit length. The lengths between the f0 and two other simulations the E1f2 and the E1f3 are $l_{f0-E1f2} = 0.172 \pm 0.0067$ and $l_{f0-E1f1} = 0.1875 \pm 0.0102$ respectively.

The lengths calculations indicate the $l_{f0-E1f1}$ to be the shortest at confidence level 0.95, which indicates E1f1 to be most similar to f0, and the E1f2 and E1f3 are less similar to f0. Recall that in the E1f1 simulation F1 is retained in the peptide, in the E1f2 simulation F2 is retained, and in the E1f3 simulation neither is retained, we thus conclude that relative to F2, F1 is significantly more crucial to the stability of the α -helix nature of H1 and, by inference, that a transient interaction altering the structure of F1 is more likely to lead to a PrPC to PrPSc conversion than a transient interaction altering the structure of F2.

Fig. 5 is here.

3.3 Results of E2 simulations

Native conformation of S1-H1-S2 has the lowest energy in simulation. Peptides in the E2 series have the same amino acid sequence but have different initial conformation. The total energy difference $\Delta E(f_n) = E(E2f_n) - E(f_0) = 41.7, 52.7, 37.9$ and 23.2 kcal/mole for $n = 1, 2, 3$ and 4 respectively, where for every case the energy is taken after the initial energy minimization and before the simulation begins. These results confirm the expectation that the native conformation of the S1-H1-S2 peptide has the lowest energy, at least compared to the initial conformations imposed on the peptide in the E2 series of simulations. This also provides a minimum necessary validation of the force field. We make a remark whose relevance will become clearer later: among the deformed peptides, E2f4 has the lowest initial energy.

H1 is unstable against modification in orientation of F1. Recall that in simulations E2f1, E2f2 and E2f3, the initial relative orientation of F1 relative H1 is changed (see Fig.2). Fig.6 shows the number of residues that constitute the α -helix in H1 as a function of simulation time in these simulations. Similarly, we apply the previous approaches to evaluate 95% confidence interval of length between the f0 and four E2 simulations, which are $l_{f0-E2f1} = 0.1006 \pm 0.0085$, $l_{f0-E2f2} = 0.0933 \pm 0.0099$, $l_{f0-E2f3} = 0.0474 \pm 0.0062$, and $l_{f0-E2f4} = 0.003 \pm 0.0014$ respectively. The results put the E2f1, E2f2, and E2f3 in an unstable class. The E2f4 and the f0 are in the stable class. It indicates that retaining F1 in the peptide but changing its orientation relative to H1 is sufficient to destabilize the structure of H1. In particular, the modification in E2f1, which has the longest length $l_{f0-E2f1}$, has the largest effect on the destabilization of H1.

Fig. 6 is here.

H1 is stable against modification in internal conformation of F1. In simulation E2f4 the connection between F1 and H1 is kept in its native state but the conformation of F1 is changed by altering the dihedral angles of Ser¹³⁵ (see Fig.2). The simulation results are shown in the E2f4 panel of Fig.6. The shortest length between the f0 and the E2f4, $l_{f0-E2f4} = 0.003 \pm 0.0014$, suggests that there is no difference between E2f4 and f0 at 95% confidence level. The inference is that modifying the internal conformation of F1 does not destabilize H1.

There are new hairpin-like turns in E2f1. Fig. 7 shows conformational transitions in f0, E2f1 (representing E2f1, E2f2 and F2f3), and E2f4 during a 200 ns simulation, where “ α -helix” includes the α -like structure α_{10} -helix. In all three cases, a bending site giving a hairpin-like structure persists around residue 157 during the full simulation. Kozin et al. in their experimental studies on the sheep PrPC peptide in solution pointed out that this turn may form a part of the β -sheet structure during conversion [20]. It is seen that f0 not only retains helical structure most of time in the H1 region (residues 144-152) but has a tendency to form additional helical structures around residues 126-134 as well. This last aspect is shared by E2f4. In contrast, E2f1 rarely has any helical structure in the 126-134 region, has several more bends in the 132-144 region and, after 80 ns, many more hydrogen-bonded turns in 144-152 and a hairpin-like turn at residue 156. This hairpin-like turn is also identified to be part of the scrapie-like structure in the in silico study by Derreumaux [11]. In addition, in the in vitro study by Megy et al., it was shown that the region 152-156, particularly at position 155, could be associated with the conversion [25], and that in PB buffer a mostly -hairpin like conformation was formed.

Fig. 7 is here.

Fig. 8 and 9 are here.

The Glu¹⁵²-Arg¹⁵⁶ distance in E2f1 is abnormally small. According to Kozin et al.'s studies, the overall stability of PrP142-166 is associated with the three salt bridges, bonds between two oppositely charged groups, in the H1 region [20]. These bridges connect the pairs of residues Glu¹⁴⁶-Arg¹⁴⁸, Asp¹⁴⁷-Arg¹⁵¹, and Glu¹⁵²-Arg¹⁵⁶. However, if one wants to stabilize an isolated H1 helical structure, Dima and Thirumalai suggest the first and the third salt bridges should be Asp¹⁴⁴-Arg¹⁴⁸ and Asp¹⁴⁸-Glu¹⁵² [12] for an isolated H1 helix. Since our goal is to study overall stability of the peptide and only residues 145 and 167 of 1AG2 differ from the peptide they studied, we will still consider analyzing the three pairs suggested by Kozin et al.'s studies. The charges on the six residues involved in the ionic interactions are delicately balanced and the initial distances between two oppositely charged groups in the residue pairs for Glu¹⁴⁶-Arg¹⁴⁸, Asp¹⁴⁷-Arg¹⁵¹, and Glu¹⁵²-Arg¹⁵⁶ have spans 1.052, 0.542, and 0.936 nm, respectively. These distances are measured from the NMR structure of the protein using the GROMACS tool g_saltbr, which computes the distance between the centers of mass of two oppositely charged groups. Notes that g_saltbr measures distance between center of mass of two oppositely charged groups. The left panel of Fig.8 shows the distance of the Glu¹⁴⁶-Arg¹⁴⁸ as a function of simulation time in the three simulations f0, E2f1 and E2f4. The histograms in the right panel gives the percentage of simulation time as a function of distance. The most likely distance in the f0 and E2f4 simulations lies in the range 0.85 to 1.05 nm, whereas for E2f1 the range is slightly greater, 0.95 to 1.1 nm. Thus the ionic bond in E2f1 is slightly weakened in E2f1 relative to the two other cases, while more rigidly confined in its range. Overall there is no significant difference among the three cases. The computed distances are broadly consistent with the NMR-measured distance of ~1.05 nm for the native conformation.

Fig.9 (right panel) shows the span of the Asp¹⁴⁷-Arg¹⁵¹ also do not vary much in the three simulations. In all case the span is concentrated within a relatively narrow range of 0.20 to 0.25 nm. The computed value is however noticeably less than the NMR-measured distance of 0.54 nm for the native conformation.

The situation shown in Fig. 10 for the Glu¹⁵²-Arg¹⁵⁶ is drastically different from the two other pairs. In the f0 and E2f4 simulations the distance is mostly in the range 0.80 to 1.20 nm, and in the range 0.15 to 0.25 nm about 10% of the time. In sharp contrast, in the E2f1 simulation, except for two transient periods, one at the beginning and one at around 70 ns, the distance is less than 0.25 nm. That the distance settles to within a narrow range of 0.20 to 0.25 nm after 75 ns of simulation may be correlated with the (faint) appearance of a hairpin-like turn at residue 156 (see Fig. 7). This distance is somewhat close to Megy et al. studies of sheep prion protein in PB buffer, which is about 0.27 nm [25]. Although our simulations does not mimic PB buffer, it seems the modification of the relative orientation of the F1 flank to reach a hairpin-like conformation around residue 152-156 similar to the Megy et al.'s discovery in PB buffer, which is believed to be likely associated with the pathogenic conversion. Namely, it may suggest the modification to be a required interaction for triggering conversation. It requires further investigations. Yet it is out of our current work's scope and will be left for future studies.

Hydrophobic does not play a major role in the unfolding of H1. The solvent accessible surface (SAS) in a peptide gives an indication of effect of the hydrophobic force on its structure. In the mouse prion 1AG2 there are nine hydrophobic residues and five non-polar Glycines (underlined) in F1: G¹²⁴LGGYMLGS AMSRPMIHFGN¹⁴²; five hydrophobic residues in F2: N¹⁵³MYRYPPNQV YYRPVD¹⁶⁷; and none in H1.

The left panel in Fig.11 shows the SAS as a function of run time in the simulations f0, E2f1 and E2f4. It is seen that in f0 the SAS mostly fluctuates around 23 nm². In E2f1, the SAS shows large fluctuation - between 18 and 26 nm² - during the first 100 nm of the simulation, suggesting major conformational changes, but settles to a narrow range of 23±2 nm² after 100 nm². In E2f4, the fluctuation is larger then in f0, but does not have the large swings seen in E2f1. These fluctuations are only partly reflected in the histograms in the right panel, which gives percentage of time against SAS. The means and standard deviations in SAS for the three cases are 22.9±1.3, 23.0±2.0, and 22.8±1.5 nm² for f0, E2f1, and E2f4, respectively. The larger standard deviation in the SAS of

Fig. 10 is here.

E2F1 is caused by the conformational fluctuation in E2f1 during the early stages of the simulation. Overall, the SAS value does not appear to be sensitive to conformational transitions in the S1-H1-S2 peptide.

Fig. 11 is here.

4 Summary and Discussion

The template-assistance model attribute the pathogenesis of prion disease to an autocatalytic process, which occurs via transient interactions between PrPC (the mouse 1AG2 peptide) with PrPSc. Motivated by a basic assumption of the model, that a transient interaction may trigger a conformation conversion, we carried out MD simulations of a simplified variant of the model. Specifically, we systematically imposed classes of simple alterations to the PrPC peptide, which served as representations of the consequences of possible transient PrPC-PrPSc interactions, and examined whether such alterations would trigger the unfolding of the H1 region of PrPC.

The reliability of the force field used in the simulations (ff03 of the AMBER 8 package [6]) was verified in several ways: relative to its conformational variants, the S1-H1-S2 peptide had the lowest simulation energy in its native conformation; if the initial conformation of the peptide was native, then it would largely retain its native conformation during simulation; the computed spans of the three charged pairs of residues were in qualitative agreement with the measure values. The only quantitative exception was with the span of the Asp¹⁴⁷-Arg¹⁵¹; a computed distance of 0.20 to 0.25 nm versus a NMR measured value of 0.54 nm.

According to various *in silico* and *in vitro* studies [13, 10, 37, 11, 25], the S1-H1-S2 peptide alone seems to be associated with the pathogenesis of the prion disease, and the disconnection of the H2-H3 segment from S1-H1-S2 seems to be a necessary condition for the latter's conversion to pathogenic form [10]. All subsequent simulations were done on the S1-H1-S2 peptide composed of residues 124 to 163, the residues beyond F2 including the H2-H3 region - residues 164-226 - were left out.

The first series of simulations on the S1-H1-S2 peptide were designed to show, of the two flanks F1 and F2, which would play a more important role in preserving the α -helical structure of H1. Four simulations were conducted: f0, the benchmark simulation on the entire peptide; E1f1, simulation on the peptide minus F2; E1f2, minus F1; E1f3, minus both the F1 and F2. The similarity analysis of these results suggested that the integrity of the helical nature of H1 depends crucially on the presence of F1 but only weakly on the presence of F2 (Fig. 4).

In the second series of tests F2 was left alone and artificial conformation alterations were made on F1 prior to simulation (Fig.2). In E2f1, E2f2, and E2f3, the relative orientations of H1 and the F1 was modified by changing the two dihedral angles of residue Asn¹⁴³ joining F1 to H1. In E2f4 the relative orientations of H1 and the F1 were unchanged while the internal native conformation of F1 was altered by changing the dihedral angles of Ser¹³⁵. It was found in the similarity analysis that keeping the F1-H1 angle intact was crucial to the integrity of the native H1 structure whereas keeping the internal structure of F1 was not (Fig. 6). We remark that the present investigation is about the transient instability of H1 after a disturbance is made to S1-H1-S2. Hence the simulation that follows is not supposed to be very long; in the present study the duration of all simulations were 200 ns. Theoretically, a sufficiently long simulation will always bring the S1-H1-S2 peptide back to its native conformation, regardless of its initial state.

Further examination of three other properties of the peptides - the existence of hairpin-like turns, the spans of charged pairs of residues, and the hydrophobic solvent accessible surface - showed results consistent with our interpretation that a (specific) change to the relative F1-H1 orientation (E2f1, or E2f3, or to a lesser extent E2f2) would cause H1 to unravel while a change in the internal conformation of F1 (E2f4) would not. The spans of all three pairs in the S1-H1-S2 peptide are similar during the f0 and E2f4 simulations. In the E2f1, the span of the Glu¹⁵²-Arg¹⁵⁶ is reduced drastically from a native value of about 1.0 nm to about 0.2 nm. This change appears to correlate

with the appearance of an additional hairpin-like turn around residue 152 in the simulation of E2f1 (after 75 ns), a feature absent in the simulations of f0 and E2f4. The SAS in the three simulations all average to about 23 nm², but in the early part of the E2f1 simulation (up to 100 ns) large fluctuation were seen, indicative of substantial conformational changes.

The conformations of 1AG2 peptide and its subunits, the S1-H1-S2 peptide and the H2-H3 domain, all turned out to be quite robust. Our simulations showed that neither the conformation integrity of S1-H1-S2 nor that of H2-H3 depends on the presence of the other. Furthermore, the native H1 conformation was robust against any changes involving F2 and changes to the internal structure of F1. This robustness is consistent with the fact that prion related diseases are not easily transmitted and rarely occur spontaneously, that is, non-infectiously. This may explain why, by and large, it afflicts only older people. Nevertheless, there does seem to be at least one type of vulnerability to this robustness: the helical structure of H1 is prone to unraveling when the S1-H1-S2 peptide suffers a large change in the relative F1-H1 orientation.

Acknowledgment

This work is partially supported by grants 93-2811-B-008-001 and 94-2112-M-008-013 from the National Science Council, Taiwan, ROC. We are grateful to the National Center for High-performance Computing for computer time and facilities. CYT appreciates technical help from HT Chen on the extraction of simulation data.

References

- [1] Aguzzi A, Sigurdson C, Heikenwaelder M (2008a) Molecular Mechanisms of Prion Pathogenesis. *Annu. Rev. Pathol.* 3:11-40.
- [2] Aguzzi A, Baumann F, Bremer J (2008b) The Prion's Elusive Reason for Being. *Annu. Rev. Neurosci.* 31:439-477.
- [3] Barducci A, Chelli R, Procacci P, Schettino V, Gervasio FL, Parrinello M (2006) Metadynamics simulation of prion protein: β -structure stability and the early stages of misfolding. *2006. J. Am. Chem. Soc.* 128:2705-2710.
- [4] Berendsen HJC, van der Spoel D, van Drunen R (1995) GROMACS: A message-passing parallel molecular dynamics implementation. *Comp. Phys. Comm.* 91:43-56
- [5] Calzolai L and Zahn R (2003) Influence of pH on NMR structure and stability of the human prion protein blobular domain. *J. Biol. Chem.* 278:35592-35596.
- [6] Case DA, Cheatham TE, Darden T, Gohlke H, Luo R, Merz Jr. KM, Onufriev A, Simmerling S, Wang B, Woods R (2005) The AMBER biomolecular simulation programs. *J. Computat. Chem.* 26:1668-1688.
- [7] Castilla J, Saá P, Hetz C, Soto C (2006) In vitro generation of infectious scrapie prions. *Cell* 121:195-206.
- [8] DeLano WL (2002) PyMOL molecular graphics system (DeLano Scientific, San Carlos, CA, USA.). <http://www.pymol.org/>.
- [9] DeMarco ML and Daggett V (2004) From conversion to aggregation: Protomembrane formation of the prion protein. *Proc. Natl. Acad. Sci. USA.* 101:2293-2298.

- [10] DeMarco ML and Daggett V (2007) Molecular mechanism for low pH triggered misfolding of the human prion protein. *Biochem.* 46:3045-3054.
- [11] Derreumaux P (2001) Evidence that the 127-164 region of prion proteins has two equi-energetics conformations with β or α features. *Biophys. J.* 81:1657-1665.
- [12] Dima RI and Thirumalai D (2004) Probing the instabilities in the dynamics of helical fragments from mouse PrP^C. *Proc. Natl. Acad. Sci. USA.* 101:15335-15340.
- [13] Eghiaian F, Grosclaude J, Lesceu S, Debey P, Doublet B, Treguer E, Rezaei H, Knossow M (2004) Insight into the PrPC \rightarrow PrPSc conversion from the structures of antibody-bound ovine prion scrapie-susceptibility variants. *Proc. Natl. Acad. Sci. USA.* 101:10254-10259.
- [14] Guex N and Peitsch MC (1997) SWISS-MODEL and the Swiss-PdbViewer: An environment for comparative protein modeling. *Electrophoresis.* 18:2714-2723.
- [15] Guilbert C, Ricard F, Smith JC (2000) Dynamic simulation of the mouse prion protein. *Biopolymers.* 54:406-415.
- [16] Harris DA (1999) Cellular biology of prion diseases. *Clin. Microbiol. Rev.* 12:429-444.
- [17] Horiuchi M and Caughey B (1999) Prion protein interconversions and the transmissible spongiform encephalopathies. *Structure Fold. Des.* 7:R231-R240.
- [18] Jackson GS and Clarke AR (2000) Mammalian prion proteins. *Curr. Opin. Struct. Biol.* 10:69-74.
- [19] Kabsch W and Sander C (1983) Dictionary of protein secondary structure: pattern recognition of hydrogen bond and geometrical features. *Biopolymers.* 22:2577-2637.
- [20] Kozin SA, Bertho G, Mazur AK, Rabesona H, Girault JP, Haertie T, Takahashi M, Debey P, and Hoa GHB (2001) Sheep prion protein synthetic peptide spanning helix 1 and β -strand 2 (Residue 142-166) shows β -hairpin structure in solution. *J. Biol. Chem.* 49:46364-46370.
- [21] Levy Y, Hanan E, Solomon B, Becker OM (2001) Helix-coil transition of PrP106-126: Molecular dynamic study. *Proteins.* 45:382-396.
- [22] Levy Y and Becker OM (2002) Conformational polymorphism of wild-type and mutant prion proteins: Energy landscape analysis. *Proteins.* 47:458-468.
- [23] Lindahl E, Hess B, van der Spoel D (2001) Gromacs 3.0: A package for molecular simulation and trajectory analysis. *J. Mol. Mod.* 7:306-317.
- [24] Malolepsza E, Boniecki M, Kolinski A, Piela L (2005) Theoretical model of prion propagation: A misfolded protein induces misfolding. *Proc. Natl. Acad. Sci. USA.* 102:7835-7840.
- [25] Megy S, Bertho G, Kozin SA, Deby P, Hoa GHB, Girault J-O (2004) Possible role of region 152-156 in the structural duality of a peptide fragment sheep prion protein. *Protein Sci.* 13:3151-3160.
- [26] Morrissey MP and Shakhnovich EI (1999) Evidence for the role of PrP^C helix 1 in the hydrophilic seeding of prion aggregates. *Proc. Natl. Acad. Sci. USA.* 96:11293-11298.
- [27] Muramoto T, Scott M, Cohen FE, Prusiner SB (1996) Recombinant scrapie-like prion protein of 106 amino acids. *Proc. Natl. Acad. Sci. USA.* 93:15457-15462.
- [28] Onufriev A, Bashford D, Case DA (2000) Modification of the generalized Born model suitable for macromolecules. *J. Phys. Chem. B* 104:3712-3720.

[29] Pan KM, Baldwin M, Nguyen J, Gasset M, Serban A, Groth D, Mehlhorn I, Huang Z, Fletterick RJ, Cohen FE (1993) Conversion of α -helices into β -sheets features in the formation of the scrapie prion proteins. Proc. Natl. Acad. Sci. USA. 90:10962-10966.

[30] Prusiner SB (1998) Prions. Proc. Natl. Acad. Sci. USA. 95:13363-13383.

[31] Riek R, Hornemann S, Wider G, Billeter M, Glockshuber R, Wuthrich K (1996) NMR structure of the mouse prion protein domain PrP. Nature. 382:180-182.

[32] Ryckaert JP, Ciccotti G, Berendsen HJC (1997) Numerical integration of the cartesian equations of motion of a system with constraints: Molecular dynamics of n-alkanes. J. Comput. Phys. 23:327-341.

[33] Santini S, Calude J-B, Audic S, Derreumaux P (2003) Impact of tail and mutations G131V and M129V on prion protein flexibility. Proteins. 51:258-265.

[34] Santini S and Derreumaux P (2004) Helix H1 of the prion protein is rather stable against environmental perturbations: molecular dynamics of mutation and deletion variants of PrP (90-231). Cell. Mol. Life Sci. 61:951-960.

[35] Sharman GJ, Kenward N, Williams HE, Landon M, Mayer RJ, and Searle MS (1998) Prion protein fragments spanning helix 1 and both strands of β -sheet (residues 125-170) show evidence for predominantly helical propensity by CD and NMR. Folding & Design. 3:313-320.

[36] Tompa P, Tusnady GE, Simon I (2002) The role of dimerization in prion replication. Biophys. J. 82:1711-1718.

[37] Watzlawik J, Sokra L, Frense D, Griesinger C, Zweckstetter M, Schulz-Schaeffer WJ, Kramer ML (2006) Prion protein helix 1 promotes aggregation but is not converted into β -sheet. J. Bio. Chem. 281:30242-30250.

[38] van der Spoel D, Lindahl E, Hess B, van Buuren AR, Apol E, Meulenhoff PJ, Tieleman DP, Sijbers ALTM, Feenstra KA, van Drunen R, Berendsen HJC (2004) Gromacs user manual version 3.2. <http://www.gromacs.org/>

[39] Zou WQ and Cashman NR (2002) Acidic pH and detergents enhance in vitro conversion of human brain PrP^{Sc} to PrP^{Sc}-like form. J. Biol. Chem. 277:43492-43947.

[40] Ziegler J, Sticht H, Marx UC, Muller W, Rosch P, Schwarzinger S (2003) CD and NMR Studies of Prion Protein (PrP) Helix 1. J. Biol. Chem. 278:50175-50181.

Figure legends

Figure 1: Left: NMR structure of C-terminal of mouse PrPC; the peptides contains three α -helices (H), two β -strands (S), and six surface loops (L). Right: The motif sequence, where the number of the leading residue in each motif is given.

Figure 2: Initial conformations of the S1-H1-S2 peptide in the E2 series of simulations. Left: the initial conformations of E2f1, E2f2, and E2f3, where the native values of the dihedral angles Asn¹⁴³'s are changed. Right: the initial conformations of E2f4, where the dihedral angles of Ser¹³⁵ are changed.

Figure 3: Left panel plots root mean square deviation (RMSD) versus simulation time. Right panel plots radius of gyration.

Figure 4: Stability of H1 in E1 simulation. The number of residues in the α -helix as a function of simulation time in three E1 simulations. Result of f0 is also shown for comparison.

Figure 5: A schematic plot of family tree for the f0 and the E1 simulations. The branch length is scale free.

Figure 6: Stability of H1 in E2 simulations. Plots show number of residues in the α -helix as a function of simulation time in E2f1, E2f2, E2f3, and E2f4.

Figure 7: Conformational transitions of the 124-167 peptide in 200 ns simulations, with initial conformations being native (f0), E2f1, and E2f4, respectively. Y-axis denotes residue number and x-axis gives simulation time. Secondary structure are color-coded as shown at the top of the figure, where 3₁₀-helix is classified as α -helix.

Figure 8: Variation with time in the span of the Glu¹⁴⁶-Arg¹⁴⁸ in the f0, E2f1, and E2f4 simulations (left panel) and percentage of time the span has a specific distance (right panel).

Figure 9: Variation with time in the span of the Asp¹⁴⁷-Arg¹⁵¹ in the f0, E2f1, and E2f4 simulations (left panel) and percentage of time the span has a specific distance (right panel).

Figure 10: Variation with time in the span of the Glu¹⁵²-Arg¹⁵⁶ in the f0, E2f1, and E2f4 simulations (left panel) and percentage of time the span has a specific distance (right panel).

Figure 11: Variation with time in the hydrophobic SAS in the f0, E2f1, and E2f4 simulations (left panel) and percentage of time the SAS has a specific value (right panel).

Figures

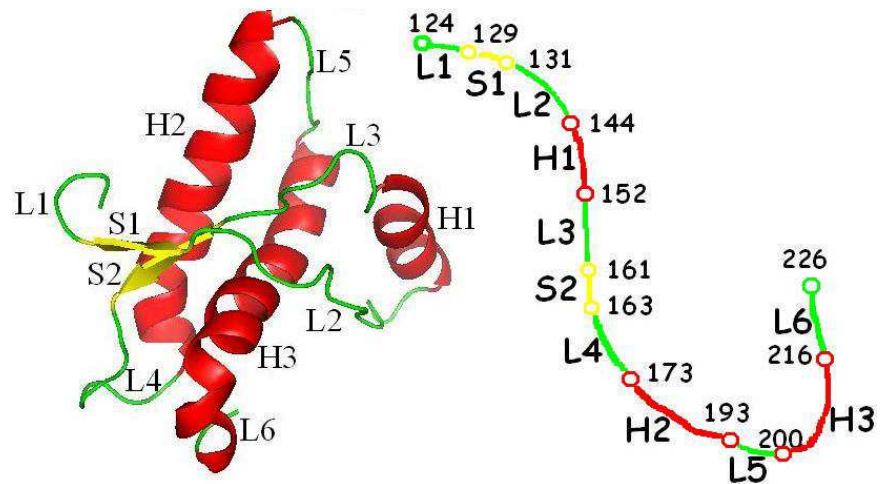


Figure 1:

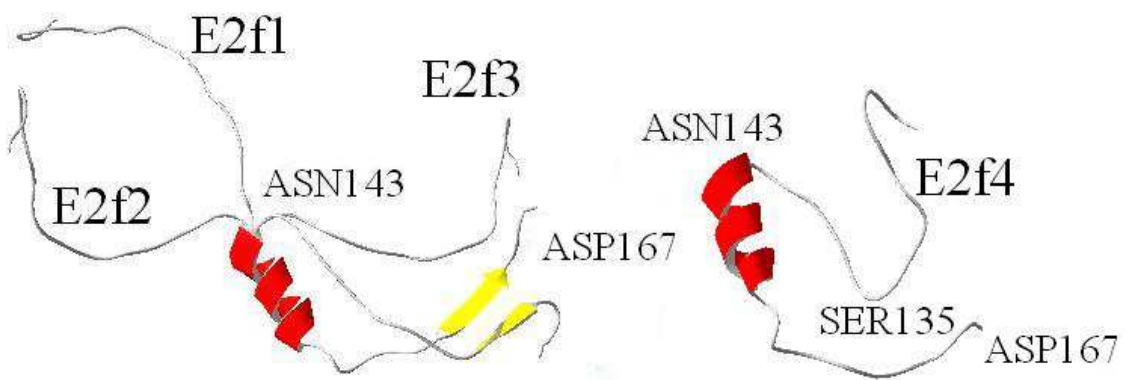


Figure 2:

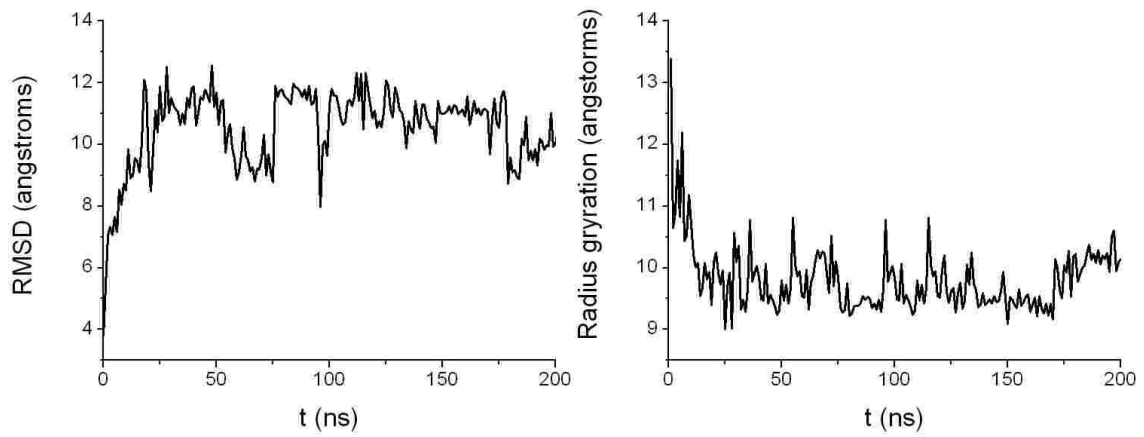


Figure 3:

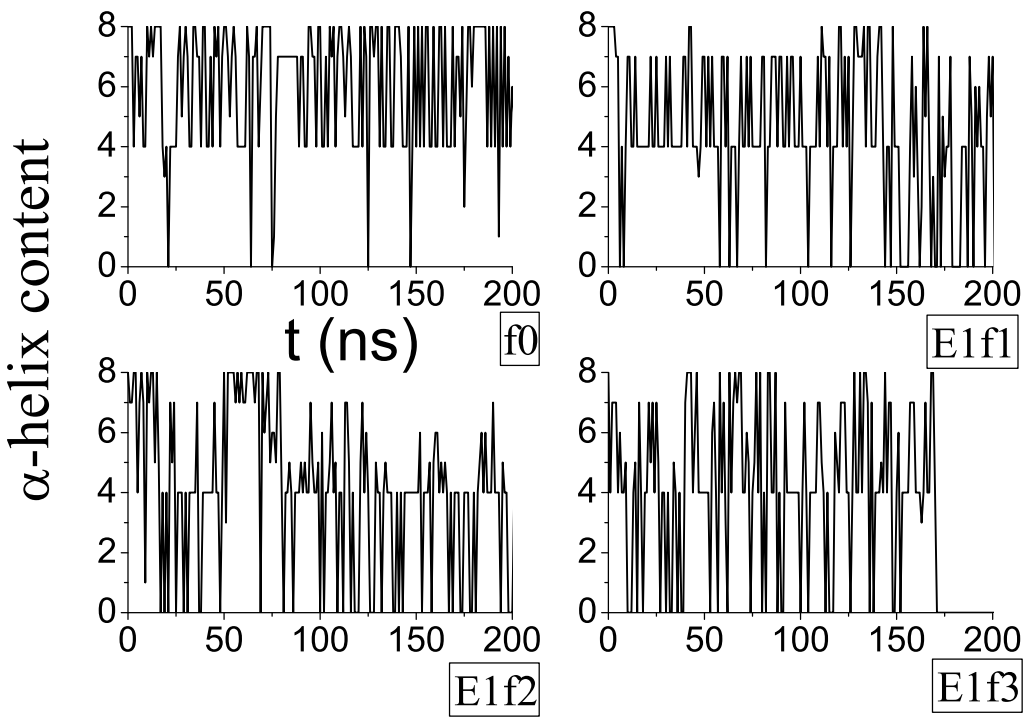


Figure 4:

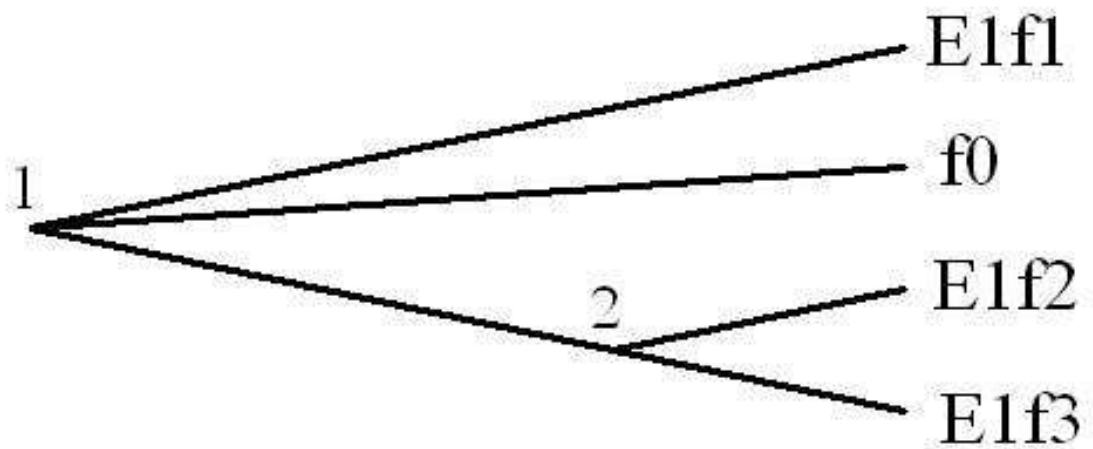


Figure 5:

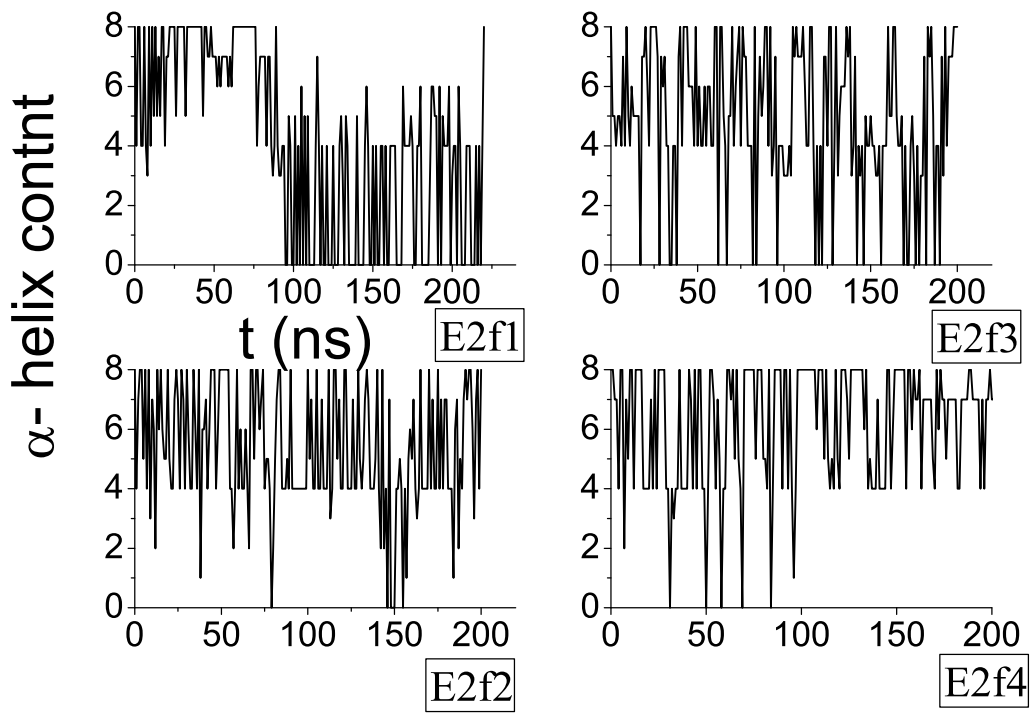


Figure 6:

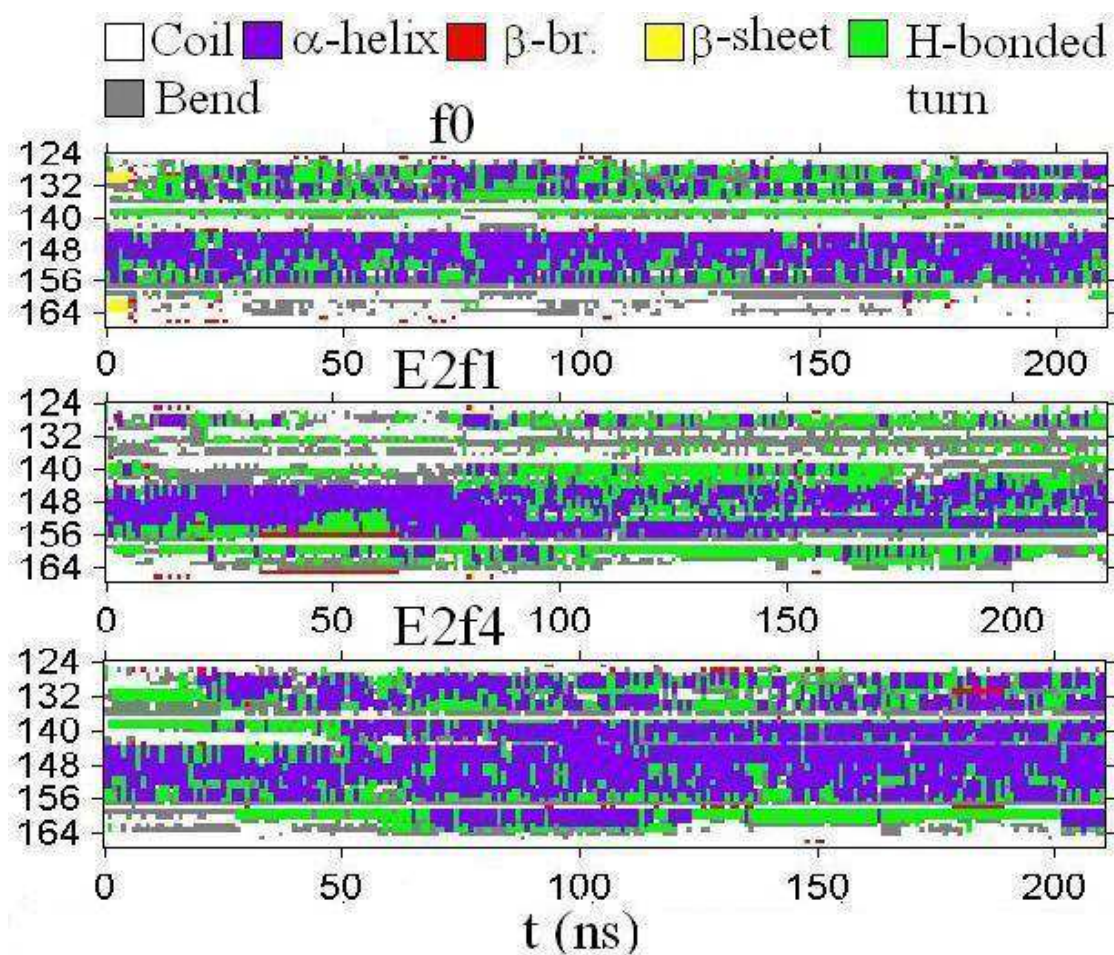


Figure 7:

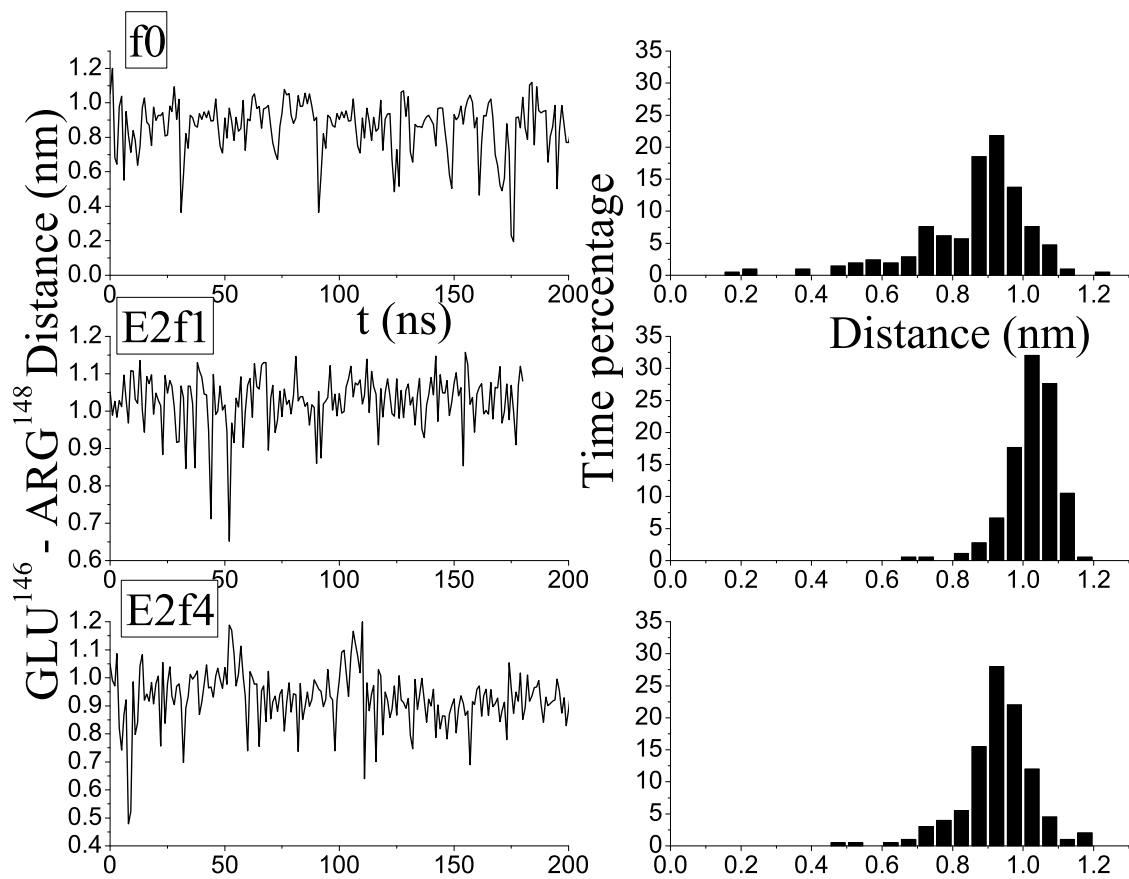


Figure 8:

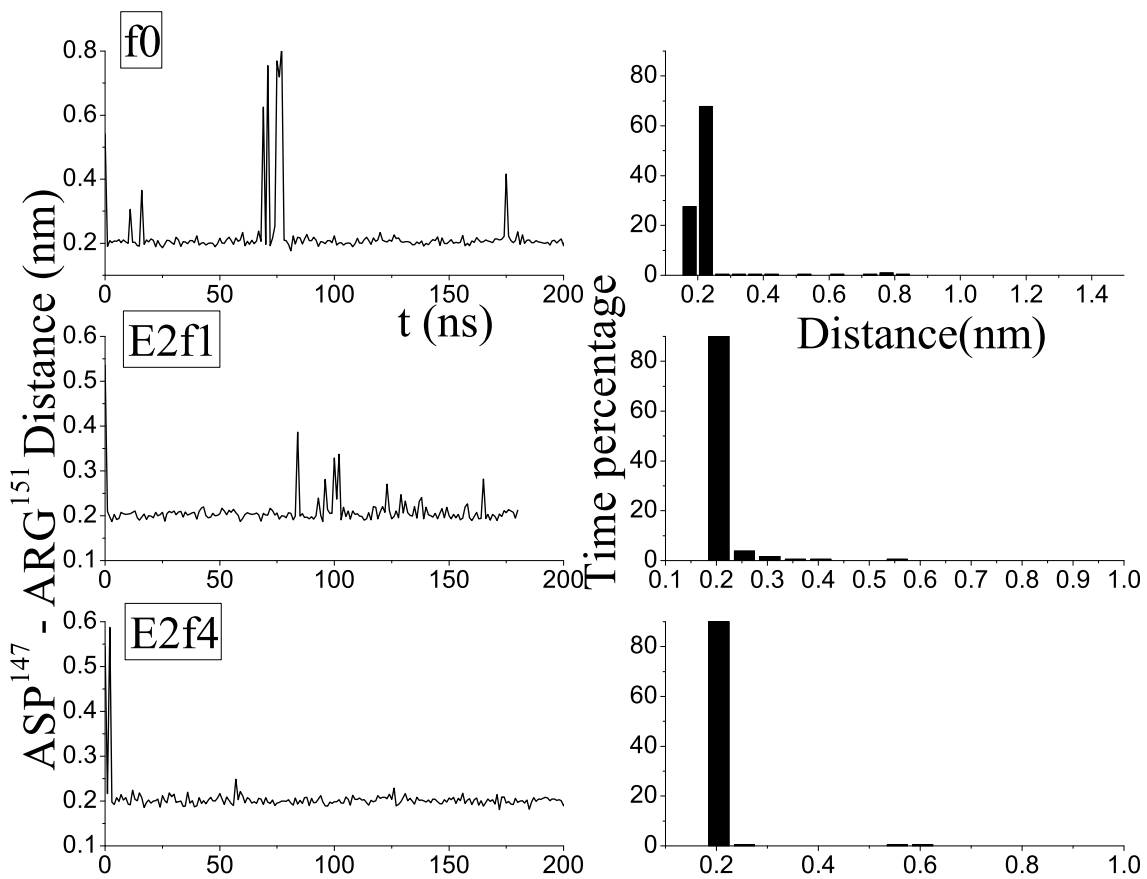


Figure 9:

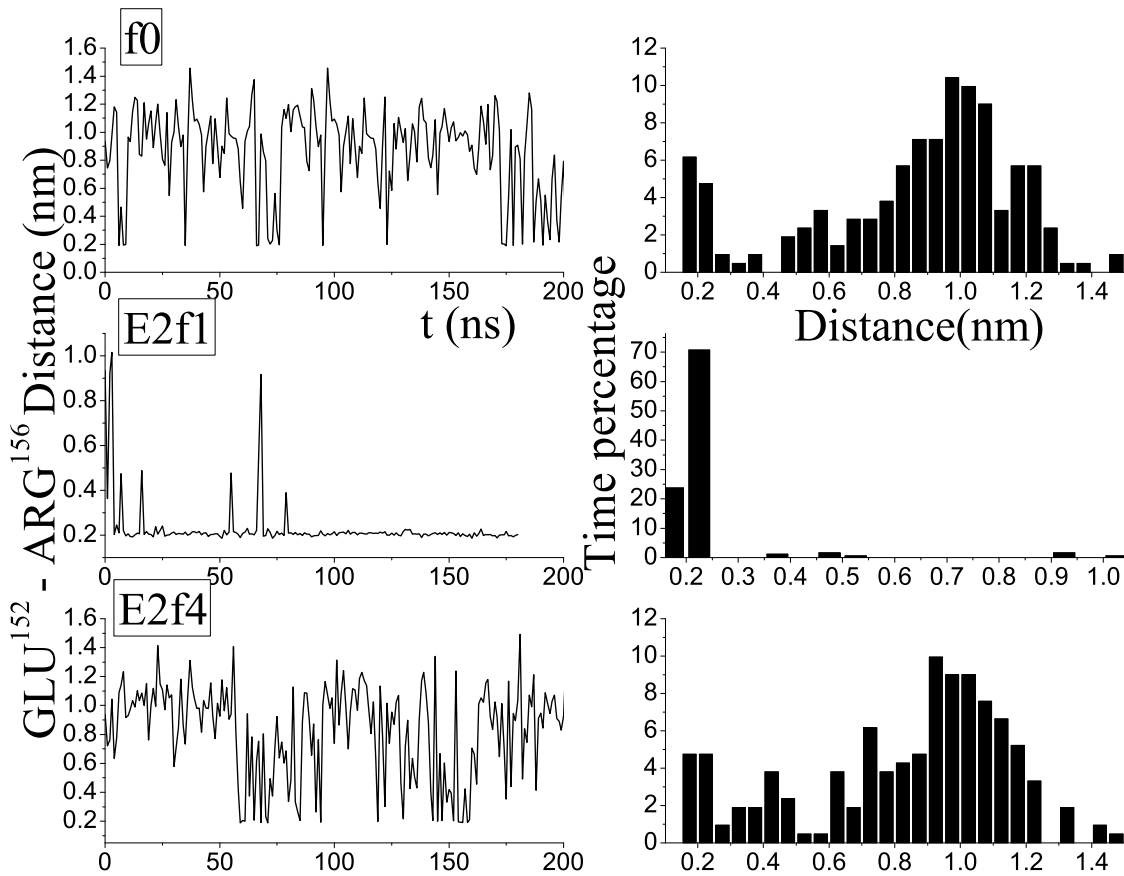


Figure 10:

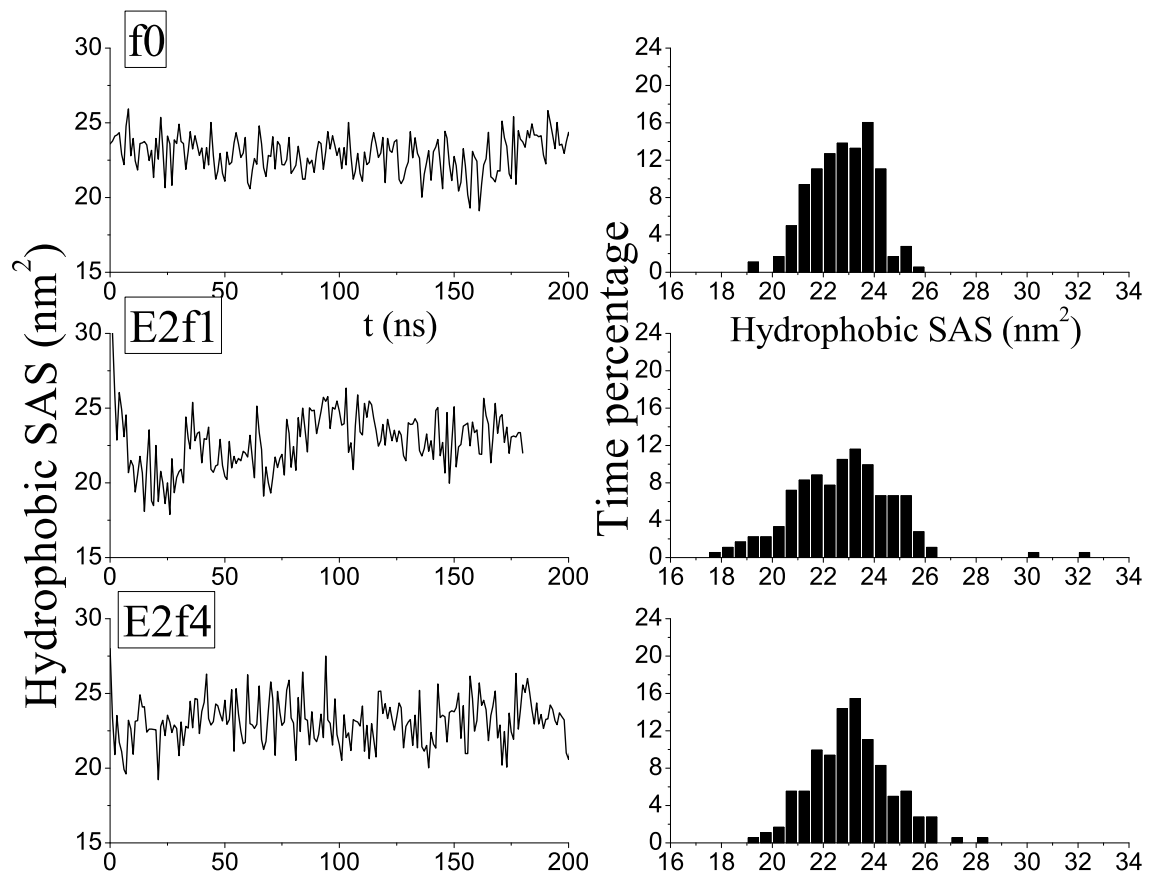


Figure 11: